Table 2 σ_x^* at $x=0$

y/h	0	0.2	0.4	0.6	0.8	1.0
σ_x^*	1.0164	0.9897	0.9777	0.9743	0.9898	1.0179

Table 3 Stress ratio τ_{xy}^*

$y/h=$	0.1	0.3	0.5	0.7	0.9
$x=0.8L$	1.0156	1.0012	0.9950	0.9968	1.0066
$x=L$	0.9150	0.9265	0.9762	1.0640	1.1900

Table 4 Stress ratio σ_y^*

$y/h=$	0.1	0.3	0.5	0.7	0.9
$x=0.8L$	0.8397	0.8388	0.8719	0.9291	0.9875
$x=L$	0.0164	0.1425	0.3750	0.6737	0.9450

Table 5 W^* at $y=0$

x/L	0	0.2	0.4	0.6	0.8
W^*	1.1068	1.1071	1.1078	1.1086	1.1089

Table 6 Displacement ratio u^*

$x/L=$	0.2	0.4	0.6	0.8	1.0
$y=0$	1.0163	1.0160	1.0148	1.0122	1.0098
$y=h$	0.6034	0.5788	0.5343	0.4723	0.4281

Numerical Results and Discussions

For illustrative purposes, $q_x=0$, $q_y=p$, and $L_1=L_2=L$ are considered. The depth h is taken to be one-quarter of a unit. Rather short beams with $L=2h$ and $4h$, simply supported at $x=\pm L$ and $y=0$ are considered. The boundary conditions at $x=L$ for 1-2-3 and 3-4-5 order theories are $N_0=N_1=W_0=0$ and $N_0=N_1=N_2=W_0=U_0'=0$, respectively.

As a first example for which $p=P_0(L-x)$, Neou's[4] Airy polynomial stress function solution is comparable to the present 1-2-3 order theory. It is found that expressions for σ_y are identical, and discrepancies for σ_x and τ_{xy} are negligible between the two analyses. While the displacements can be calculated or be prescribed as boundary conditions in the present analysis, they can not be easily included in Ref. 4.

As a second example, $p=$constant is considered. Results based on 1-2-3 and 3-4-5 order theories will be discussed. As the discrepancies between these two theories increase as the beam length decreases, comparison of numerical results for the shorter beam $L=2h$ will be given. Longitudinal stresses of σ_x calculated according to the 3-4-5 order theory are slightly lower than those of 1-2-3 order theory for $0.2h\le y\le 0.8h$, and reversed in the remaining portion. Some results of σ_x^* at $x=0$, with the superscript * denoting the ratio of the quantity based on 3-4-5 order theory to that of 1-2-3 order theory, are listed in Table 2. Results for the shearing stress τ_{xz} calculated according to both theories agree very well in most of the interior part of the beam. Deviation begins at approximately $x=0.8L$. In this region near the edge, some results on the stress ratio τ_{xy}^* are given in Table 3. Results on σ_y agree well for most of the interior region. They begin to deviate at approximately $x=0.6L$ for the shorter beam. While σ_y does not vary along the x axis for 1-2-3 theory, it generally exhibits sharp stress gradients near the beam edge according to the 3-4-5 order theory. Some results on the stress ratio σ_y^* are listed in Table 4.

While w does not vary through the beam thickness for the 1-2-3 order theory, the variation is also very small according to 3-4-5 order theory. Results on the displacement ratio w^* along $y=0$ are given in Table 5.

Results on u based on 1-2-3 and 3-4-5 order theories agree well for the lower portion, but deviate from each other in the upper portion of the beam. Deviations become larger for sections closer to the edge. The discrepancies at $y=h$, quite significant for the shorter beam, are evident in the results in Table 6 on the displacement ratio u^*.

Acknowledgment

The work forms part of a study in a Special Problems course, ESM 8503, at Georgia Institute of Technology.

References

[1]Sokolnikoff, I. S., *Mathematical Theory of Elasticity*, McGraw-Hill Book Company, New York, 1956.

[2]Timoshenko, S. and Goodier, J. N., *Theory of Elasticity*, McGraw-Hill Book Company, New York, 1951.

[3]Dym, C. L. and Shames, I. H., *Solid Mechanics: A Variational Approach*, McGraw-Hill Book Company, 1973.

[4]Neou, C. Y., "Direct Method for Determining Airy Polynomial Stress Functions," *Journal of Applied Mechanics, Transactions of ASME*, Vol. 24, 1957, pp. 387-390.

Conservative Implicit Method for Shock Wave Calculations

Sambasiva R. Mulpuru* and Sanjoy Banerjee†
Engineering Physics Department, McMaster University, Hamilton, Ontario, Canada

Nomenclature

A	= cross-sectional area of a node
e	= internal energy in a node
ℓ	= length of a node
m	= flow Mach number
M	= mass in a node
P	= pressure
u	= velocity defined by $(W/\rho/A)$
U	= $e+\frac{1}{2}Mu^2$; total energy in a node
V	= volume of node
W	= mass flow rate
γ	= ratio of specific heat
ρ	= density
Subscripts	
j,k,l,m	= values at positions shown in Fig. 1
0	= upstream value

Introduction

NUMERICAL techniques for calculations in which shock waves undergo considerable change from a state of initial steady propagation are of interest in many situations. For example, the interaction of a normal shock wave with a discontinuous area constriction results in reflected and

Received June 14, 1978; revision received Dec. 13, 1978.
Copyright© American Institute of Aeronautics and Astronautics, Inc., 1978. All rights reserved.
Index categories: Computational Methods; Shock Waves and Detonations.

*Postdoctoral Fellow; presently, Atomic Energy of Canada Limited, Pinawa, Manitoba.

†Professor.

transmitted shock waves, a contact discontinuity, and expansion waves. The resulting wave pattern, as discussed by Rudinger,[1] depends upon the incident wave strength and the severity of the constriction. Many numerical methods exist in the literature that successfully calculate[2-6] the propagation of shock waves. Some of these methods use artificial dissipative terms to spread the shock discontinuity over a few grid intervals and alleviate oscillations that might otherwise arise. The artificial terms introduce little error in calculating the propagation of a steady shock; but, they are known to cause errors[7] when the shock undergoes change from one steady state to another. As the shock wave incident on an area constriction undergoes considerable change from its initial steady propagation, methods using the artificial dissipative terms are ill-suited for this and similar problems.

In this Note, we present an accurate calculation of a shock wave interaction with discontinuous area constrictions by using an implicit method to solve ordinary differential equations derived from the control volume integration of the equations in the conservation-law form. As far as we know, this particular method has not been previously applied to shock wave calculations. The method does not require addition of artificial dissipative and dispersive terms and yields a smooth (monotone) shock profile with no oscillations.

Method

The conservation equations are derived for control volumes using the "donor cell" approach of Gentry et al.[8] in which the fluid properties are defined at the control volume centers and the mass flow rates at the control volume edges. This results in a system where the control volume for the momentum conservation equation is staggered with regard to the control volume for the mass and energy conservation equations, as shown in Fig. 1. The staggered control volume approach has also been widely used in computer codes for calculating transient subsonic internal flow in nuclear reactors.[9-11]

The momentum conservation equation may be derived by integrating the stream tube momentum equation over the appropriate control volume shown in Fig. 1. Moore et al.[12] have suggested that the following approximations are good over a wide range of problems:

1) The fluid properties immediately adjacent to the discountinuous area change (at $j+$ and $j-$) are related to each other through isentropic expressions.

2) The speed of sound immediately downstream of the area change is equal to its value immediately upstream, i.e., the speed of sound at $j+$ is equal to that at $j-$ for the flow direction shown in Fig. 1.

The momentum conservation equation is then:

$$I_j \frac{dW_j}{dt} = \frac{1}{A_j^2}\frac{W^2}{\rho}\Big)_k - \frac{1}{A_\ell^2}\frac{W^2}{\rho}\Big)_\ell + S_j(P_k - P_\ell) + S_j\left[\frac{|W_j|^2}{\rho_0 A_0}\left\{\frac{\rho}{\rho_0}\left(\frac{m^2}{m_0^2}+\frac{1}{m_0^2}\right)-\left(1+\frac{1}{m_0^2}\right)\right\}\right] \quad (1)$$

where

$$I_j = \left[\left(\frac{\ell}{A}\right)_k + \left(\frac{\ell}{A}\right)_\ell\right]\Big/2 \text{ and } S_j = W_j/|W_j|$$

The subscript 0 indicates the value immediately upstream of the area change and no subscript indicates the value immediately downstream; i.e., at $j-$ and $j+$, respectively, for the flow direction shown in Fig. 1. The first two terms on the right-hand side of Eq. (1) contain the mass flow W at node centers. However, the mass flows are not defined at the node centers, but only at the node edges. We have used two methods of defining these values. In the first, the "upwind" value is used; i.e., for the flow direction in Fig. 1, $(W/\rho)_k$ is set equal to W_{j-1}/ρ_m and $(W/\rho)_\ell$ to W_j/ρ_k. In the second, W_k and W_ℓ are taken to be the arithmetic average of the values at the node edges; i.e., $(W/\rho)_k = (W_{j-1}+W_j)/(2\rho_k)$ and $(W/\rho)_\ell = (W_j + W_{j+1})/(2\rho_\ell)$. Calculations with both methods yield very little difference in results for the cases discussed in this paper. For certain problems, the first method is more numerically stable than the second.

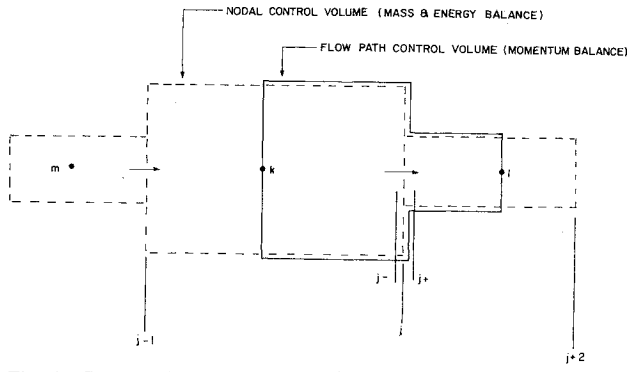

Fig. 1 Staggered control volumes for mass, energy, and momentum balances.

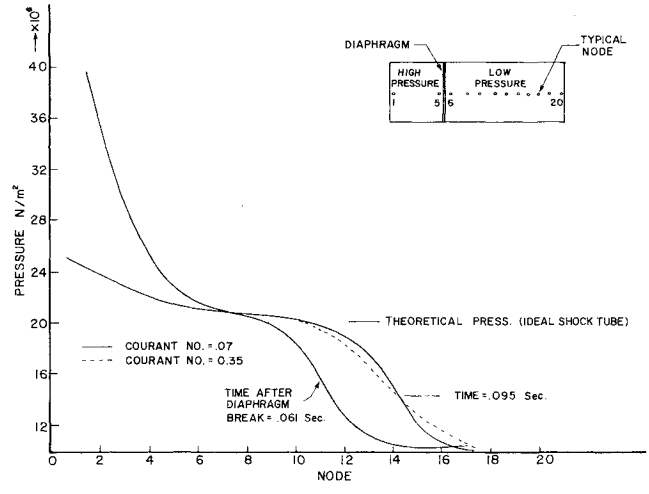

Fig. 2 Pressure history in shock tube after diaphragm rupture. Initial high pressure = 4.34 atm, low pressure = 1.0 atm, and temperature = 300 K; $\gamma = 1.4$. Theoretical Mach number = 1.37; computed Mach number = 1.39.

Integration of the energy and mass equations over the appropriate control volume (shown in Fig. 1) yields

$$\frac{dU_k}{dt} = \frac{U+P/\rho}{M}\Big)_0 W_{j-1} - \frac{U+P/\rho}{M}\Big)_0 W_j \quad (2)$$

$$\frac{dM_k}{dt} = W_{j-1} - W_j \quad (3)$$

The equation of state relates pressure to internal energy and density. For an ideal gas, it is:

$$P_k = (\gamma - 1)/V_k[U_k - \tfrac{1}{2}M_k \cdot \bar{W}_k^2/(\rho_k/A_k)^2] \quad (4)$$

where

$$\bar{W}_k^2 = (|W_{j-1}|^2 + |W_j|^2)/2$$

Equations (1-3) for all the control volumes in the system may be represented by the vector equation

$$\frac{d\tilde{y}}{dt} = \tilde{f}(t,\tilde{y}) \quad (5)$$

Using the Euler implicit method, the following set of nonlinear algebraic equations is obtained:

$$\tilde{y}^{n+1} = \tilde{y}^n + \Delta t \tilde{f}^{n+1} \tag{6}$$

where the superscript n denotes values of the vectors at time-step n.

Application of the Newton-Raphson method to solve the nonlinear system, Eq. (6), iteratively yields

$$[\tilde{I} - \Delta t \partial \tilde{f}(\tilde{y}_i^{n+1}) / \partial \tilde{y}_i^{n+1}](\tilde{y}_{i+1}^{n+1} - \tilde{y}_i^{n+1})$$
$$= -\tilde{y}_i^{n+1} + \Delta t \tilde{f}(\tilde{y}_i^{n+1}) + \tilde{y}_i^n \tag{7}$$

where $\tilde{I}$ is the identity matrix, subscript i indicates the initial values of the vector $\tilde{y}$ and subscript $i+1$ indicates improved values after one iteration. $\partial \tilde{f}(\tilde{y}_i^{n+1}) / \partial \tilde{y}_i^{n+1}$ is the Jacobian taken over all control volumes in the system. The number of iterations necessary depends on the rapidity of the transient, the convergence criterion, and the Courant numbers (the values of $(|W/\rho A| + a)\Delta t/\Delta x$). For the problems and Courant number used in this study,

$$|\tilde{y}_2^{n+1} - \tilde{y}_1^{n+1}| / \tilde{y}_1^{n+1} < 10^{-4} \tag{8}$$

The method is stable at time-steps well over those leading to a Courant number of one. This is expected in view of Porshing's[14] study of the stability characteristics of implicit methods for the solution of the equations in conservation law form.

Results

The method described has been used for calculation of shock wave propagation in an ideal shock tube and shock wave interaction with discontinuous area changes. In general, the calculations for the second case are quite difficult, especially with regard to the reflected shock strengths.

The results of the shock tube calculations are shown in Fig. 2 for two Courant numbers. As evident, the shock pressure ratio and velocity are well predicted. The shock spread, also characteristic of methods using explicit artificial viscosity, indicates the inherent dissipation in the numerical method. The dissipation and, hence, the shock spread may be controlled by controlling the Courant number.

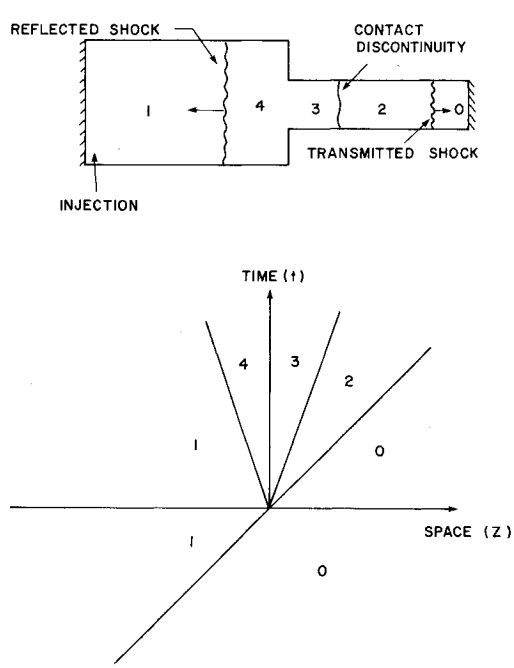

Fig. 3 Shock wave interaction with an area reduction.

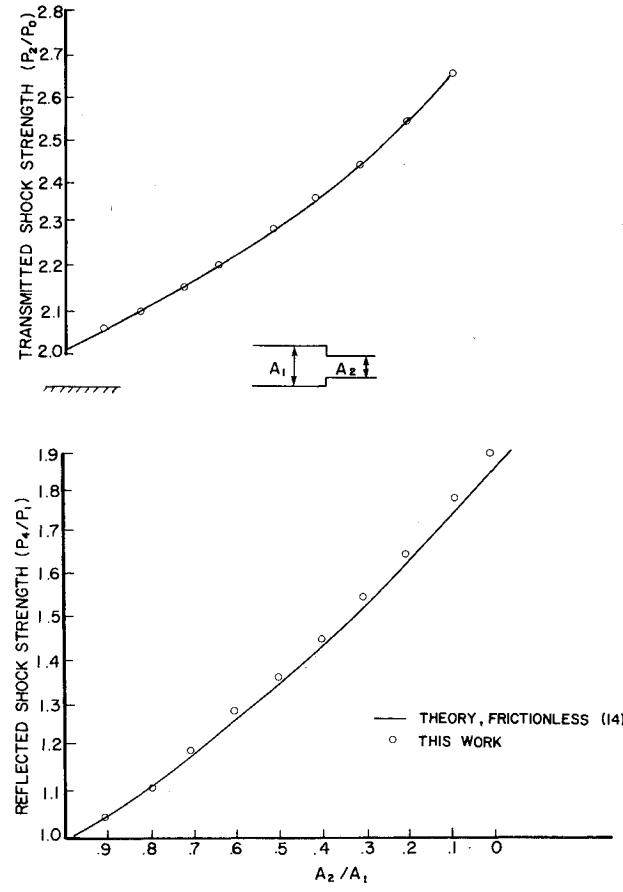

Fig. 4 Comparison of transmitted and reflected shock strengths for varying area ratios. Incident shock strength (P_1/P_0) = 2.0; γ = 1.4.

For calculation of shock wave interactions with area changes, the problem geometry was of the form shown in Fig. 3. The shock wave is set in motion at the left-hand side. The amplitude of the shock wave can be controlled by the injection rate. The wave pattern resulting from a shock interaction with a discontinuous area reduction is shown in Fig. 3.

The interface of regions 0-1 indicates the incident shock path. The other interfaces 0-2, 4-1, and 2-3 represent the paths of the transmitted shock, reflected shock, and contact discontinuity, respectively. By using injection for the shock wave rather than a shock tube, the expansion wave is eliminated. This facilitates the examination of the steady-state properties at the area change (regions 3 and 4 in Fig. 3).

The strengths of the reflected (P_4/P_1) and transmitted (P_2/P_0) shock waves arising out of the interaction of an incident shock wave with a wide range of area reductions are shown in Fig. 4. The theoretical values for frictionless flow shown in the figure were calculated from the work of Reichenbach and Dreizler.[14] The results obtained show that the strength of the reflected shock and transmitted shock are well predicted by the numerical calculations.

Conclusions

A control volume integration approach that conserves mass and energy exactly, together with an implicit solution method, has been applied to shock wave calculations. The method has sufficient inherent dissipation and explicit artificial viscosity terms are not required to damp oscillations. Shock spread can be controlled by controlling the Courant number.

The method gives good results even when the shock undergoes considerable change, such as during interactions with discontinuous area changes. It can be applied relatively easily to complex one-dimensional systems and should be useful for calculations of this type.

References

[1] Rudinger, G., *Nonsteady Duct Flow: Wave Diagram Analysis*, Dover Publications, New York, N.Y., 1969.

[2] von Neumann, J. and Richtmeyer, R. D., "A Method for the Numerical Calculation of Hydrodynamical Shocks," *Journal of Applied Physics*, Vol. 21, March 1950, pp. 232-257.

[3] Landshoff, R., "A Numerical Method for Treating Fluid Flow in the Presence of Shocks," LASL Rept. LA-1930, Los Alamos Science Lab., University of California, Jan. 1955.

[4] Longley, H. C., "Methods of Differencing in Eulerian Hydrodynamics," LASL Rept. LAMS-2379, 1960, Los Alamos Science Lab., University of California, April 1960.

[5] Rusanov, V. V., "Calculation of Interaction of Non-steady Shock Waves with Obstacles," *Zhur. Vychishitel'noi Mathematicheskoi Fiziki*, Vol. 1, No. 2, 1961, pp. 267-279.

[6] van Leer, B., "Stabilization of Finite Difference Schemes for the Equations of Inviscid Compressible Flow by Artificial Diffusion," *Journal of Computational Physics*, Vol. 3, 1969, pp. 473-485.

[7] Cameron, I. G., "An Analysis of the Errors caused by using Artificial Viscosity Terms to Represent Steady State Shock Waves," *Journal of Computational Physics*, Vol. 7, No. 7, 1966, pp. 1-20.

[8] Gentry, R. A., Martin, R. E., and Daly, B. J., "An Eulerian Differencing Method for Unsteady Compressible Flow Problems," *Journal of Computational Physics*, Vol. 7, 1966, pp. 87-118.

[9] Moore, K. W. and Rettig, W. H., "RELAP4—A Computer Program for Transient Thermal-Hydraulic Analysis," Aerojet Nuclear Co. Rept. ANCR 1127, Idaho Falls, Idaho, Dec. 1973.

[10] Brittain, I. and Fayers, F. J., "A Review of U.K. Developments in Thermal-hydraulic Method for Loss of Coolant Accidents," paper presented at the OECD/NEA specialist' Meeting on Transient Two-Phase Flow, Toronto, Ontario, Aug. 1976.

[11] Arrison, N. L., Hancox, W. T., Sulatisky, M. T., and Banerjee, S., "Blow-down of a Recirculating Loop with Heat Addition," *Heat and Fluid Flow in Water Reactor Safety*, Mechanical Engineering Publications Ltd., London, 1977, pp. 77-82.

[12] Moore, K. V., Slater, C. E., Yabarrondo, L. J., and Green, G. E., "Momentum Flux Terms in Transient Hydraulic Codes," paper presented at Topical Meeting on Water Reactor Safety, U.S. Atomic Energy Commission, Technical Information Center, Washington, D.C., March 1973.

[13] Porshing, T. A., "Time-dependent Non-linear Networks," *SIAM Journal of Applied Mathematics*, Vol. 18, June 1970, pp. 861-871.

[14] Reichenbach, V.H. and Dreizler, H., "Uber den Querschmitt Sanderungen und Gitter in Kanalen anf Stosswellen," *Zeitschrift für Angenwandte Physik*, Vol. 12, June 1960, pp. 62-71.

From the AIAA Progress in Astronautics and Aeronautics Series..

OUTER PLANET ENTRY HEATING AND THERMAL PROTECTION—v. 64

THERMOPHYSICS AND THERMAL CONTROL—v. 65

Edited by Raymond Viskanta, Purdue University

The growing need for the solution of complex technological problems involving the generation of heat and its absorption, and the transport of heat energy by various modes, has brought together the basic sciences of thermodynamics and energy transfer to form the modern science of thermophysics.

Thermophysics is characterized also by the exactness with which solutions are demanded, especially in the application to temperature control of spacecraft during long flights and to the questions of survival of re-entry bodies upon entering the atmosphere of Earth or one of the other planets.

More recently, the body of knowledge we call thermophysics has been applied to problems of resource planning by means of remote detection techniques, to the solving of problems of air and water pollution, and to the urgent problems of finding and assuring new sources of energy to supplement our conventional supplies.

Physical scientists concerned with thermodynamics and energy transport processes, with radiation emission and absorption, and with the dynamics of these processes as well as steady states, will find much in these volumes which affects their specialties; and research and development engineers involved in spacecraft design, tracking of pollutants, finding new energy supplies, etc., will find detailed expositions of modern developments in these volumes which may be applicable to their projects.

Volume 64—404 pp., 6 × 9, illus., $20.00 Mem., $35.00 List
Volume 65—447 pp., 6 × 9, illus., $20.00 Mem., $35.00 List
Set—(Volumes 64 and 65) $40.00 Mem., $55.00 List

TO ORDER WRITE: Publications Dept., AIAA, 1290 Avenue of the Americas, New York, N.Y. 10019